American Mineralogist, Volume 78, pages 753–761, 1993

The determination of the O content of diamond by microactivation

E. A. Mathez
Department of Mineral Sciences, American Museum of Natural History, New York, New York 10024, U.S.A.
J. D. Blacic
Geology and Geochemistry Group, Earth and Environmental Sciences Division, Los Alamos National Laboratory, Los Alamos, New Mexico 87545, U.S.A.
C. Maggiore, T. E. Mitchell
Center for Materials Sciences, Los Alamos National Laboratory, Los Alamos, New Mexico 87545, U.S.A.
R. A. Fogel
Department of Mineral Sciences, American Museum of Natural History, New York, New York 10024, U.S.A.

Abstract

A microactivation technique has been developed to determine the O content of diamond. The target is bombarded with an energetic beam of $^{3}He^{2+}$ from a tandem accelerator to generate the reaction $^{16}O(^{3}He,p)^{18}F$. The ^{18}F decays to ^{18}O ($t_{1/2}$ = 109.8 min) by positron emission, and the decay activity is measured by coincidence counting. For most experiments the ^{3}He beam was focused to diameters of 300–800 μm, which essentially defines analytical spatial resolution, since the analytical depth is only $\approx$8 μm. The technique gives consistent results and can be used to determine O contents of diamond to concentrations of $<$5 ppm (atomic). Errors vary from 14 to 19% for concentrations of $<$100 ppm.

Most of the 28 diamond samples analyzed contain 10–100 ppm O (atomic) in spots that upon subsequent microscopic examination were found to be free of inclusions, cracks, and other defects. No other elements, such as those that would suggest that O is present in submicroscopic mineral inclusions, are associated with the O. However, in several samples with higher concentrations the O is believed to be localized in submicroscopic cracks. The analyzed samples are from the kimberlites of Monastery and Finsch, South Africa; Orapa, Botswana; Muji Mayi, Zaire; and unknown localities. They include natural types I and IIa diamond, a yellow synthetic diamond sample, and samples from which both eclogitic and peridotitic mineral inclusions had been extracted. Among them are two that contained inclusions of the reduced phase SiC. No systematic relationships of O content with location, diamond type, or inclusion association are evident. In particular, the SiC-bearing diamond is not depleted in O compared with the other diamond samples. Dislocation densities of two type IIa diamond samples were determined by TEM. It was found that there are not enough dislocations or defects to account for all the O in such diamond samples, indicating that O is present in the diamond structure. The diamond samples were also analyzed by FTIR spectroscopy. The spectra contain no bands indicative of C-O bonds. It is hypothesized that O is present in interstitial sites in the diamond structure and, on the basis of the analogy with synthetic diamond and other substances that undergo faceted growth, that the O content of diamond is controlled primarily by the kinetics of the growing surface rather than by equilibrium thermodynamic conditions or crystal defect structure.

Introduction

Diamond has the potential for providing unique information about the mantle. Studies of mineral inclusions indicate that some diamond is $>$3 b.y. in age and much older than its kimberlite host rock (Richardson et al., 1984), some having crystallized at depths exceeding 350 km (Moore and Gurney, 1985), and yet other diamond having crystallized under much more reducing conditions than generally believed to exist in the deep Earth (Moore et al., 1986; Meyer and McCallum, 1986; Leung, 1990). Diamond exhibits a wide range of isotopic composition, having $\delta^{13}C$ values from -35 to $+3$‰ (e.g., Deines, 1980; Galimov, 1991). For some suites, isotopic composition appears to be systematically related to mineral inclusion type, implying gross compositional differences among the diamond source regions (Galimov, 1991). Diamond also exhibits wide ranges in properties such as color, UV and IR absorption, and thermal and electrical conductivities, which indicate variable conditions of growth.

0003–004X/93/0708–0753$02.00

Although diamond is essentially a pure substance, some of the variability in its physical properties is due to the incorporation of small quantities of impurity elements. N is by far the most abundant impurity in diamond, affecting color and other spectroscopic properties (e.g., Bibby, 1982); B is present in some natural stones and plays an important role in determining electrical properties (e.g., Gildenblat et al., 1991), and H is probably present in the bulk of most, if not all, type I diamond (e.g., Woods and Collins, 1983). In addition, Sellschop et al. (1978, 1979, 1980) and Sellschop (1979) have suggested that O may be a major structural impurity. The presence of these impurities raises a question about their geochemical significance, such as the conditions under which diamond forms with elevated N contents.

These same questions may be posed for O. Mantle oxidation state is important because O activity exerts a fundamental control on the stabilities of mantle fluids and carbonaceous minerals (e.g., Eggler and Baker, 1982) and may influence partial melting and other petrogenetic processes (Green et al., 1987; Taylor and Green, 1987). Little is known about O in diamond, and methods for in situ analysis of O in microregions of materials at concentration levels of <100 ppm are not well developed. There are several potential ways of accomplishing such an analysis. In principle SIMS (secondary ion mass spectroscopy) should be of sufficient sensitivity. However, attempts to apply SIMS to this specific problem either have been unsuccessful (R. Hervig, personal communication) or yielded O contents of optically clear type IIa diamond of hundreds of parts per million and are thus suspect (R. G. Wilson, personal communication). There are several nuclear techniques for O analysis. For example, the utility of the reaction $^{16}O(d,p)^{17}O$ has been investigated (Borders and Harris, 1978) and applied to the analysis of O in pyrrhotite (Graham and McKenzie, 1987). We investigated this and other nuclear reactions but found them not to be of sufficient sensitivity for diamond studies.

The purposes of this communication are to describe a microactivation technique for the determination of the O content of diamond, to determine the amounts of O typically present in diamond, and to evaluate the utility of O-bearing diamond as an indicator of the O activity attendant on its formation. Our analyses indicate that diamond typically contains several tens of parts per million of O in the diamond structure, that larger quantities are present in some diamond, and that O contents are controlled in part by dislocation structure and detailed growth mechanism and not simply macroscopic, thermodynamic properties.

Analytical method

Principle

O concentration was determined by microactivation. Diamond was bombarded with an energetic beam of $^3He^{2+}$ produced by the tandem accelerator of the Ion Beam Materials Laboratory of Los Alamos National Laboratory. The nuclear reactions in diamond are

$$^{12}C(^3He,\alpha)^{11}C \rightarrow {}^{11}B \quad (1)$$

$$^{16}O(^3He,p)^{18}F \rightarrow {}^{18}O \quad (2)$$

where both ^{18}F and ^{11}C decay by positron emission to their respective daughter nuclei. Positron annihilations were counted by coincidence NaI detectors. The decay activity is accompanied by a background, which was assumed to be constant over time. The decay activity data (Fig. 1) may be represented by a function of the form

$$y = A \exp(-b_1 t) + B \exp(-b_2 t) + C \quad (3)$$

where A, B, and C are unknowns, b_1 and b_2 are the rate constants for ^{11}C and ^{18}F decay, respectively, t is time, and y is yield (counts per unit time). The respective half-lives of ^{11}C and ^{18}F are 20.39 min [1.223×10^3 s; $b_1 = (\ln 2)/1.223 \times 10^3 = 0.566\,575/10^3$ s] and 109.77 min (6.586×10^3 s; $b_2 = 0.105\,237/10^3$ s). Substitution yields

$$y = A \exp(-0.566\,575t) + B \exp(-0.105\,237t) + C. \quad (4)$$

Here t is the elapsed time from the beginning of counting expressed in units of 10^3 s. A, B, and C are the intercepts at $t = 0$ and represent the counts per 10^3 s caused by the decay of ^{11}C and ^{18}F and by the background, respectively (Fig. 1). Expression 4 is the sum of three independent expressions, and the intercepts may be determined simultaneously by nonlinear least-squares fitting.

Computation of concentration

The yield, y, is the decay activity from saturated activation computed for the time midway between the beginning and end of activation (t_i). It is related to B and the time at which counting was begun (t_0) by

$$\ln y = \ln B - 0.105\,237\,(t_0 - t_i) \quad (5)$$

and is proportional to the O content of the diamond, C_d (in atomic fraction, assumed to be constant with depth, x), by

$$y = (Q)(C_d) \int \phi_d(x)\, dx \quad (6)$$

where Q is the accumulated $^3He^{2+}$ beam charge on the diamond target, $\phi_d(x)$ is the activation cross section for Reaction 2, and x is depth. The variation of the cross section of Reaction 2 with ^3He energy is shown in Figure 2A. It is evident that the energy of the beam reaching the sample surface must be known accurately. The integrated activation cross section (Fig. 2B) was computed from the reaction cross section and the variation of ^3He energy with a range in the target. This term is unique for each target material and therefore represents a matrix correction. However, the integrated activation cross sections of diamond and Al_2O_3, which were used as the standard, differ from each other by only 6% at 4.5 MeV, making the magnitude of the correction small. Also, because the correction is expressed as a ratio of stopping powers, it is known precisely. There are no other matrix corrections. The range was computed from ion stopping powers with the program Trim (Ziegler et al., 1985). A consequence

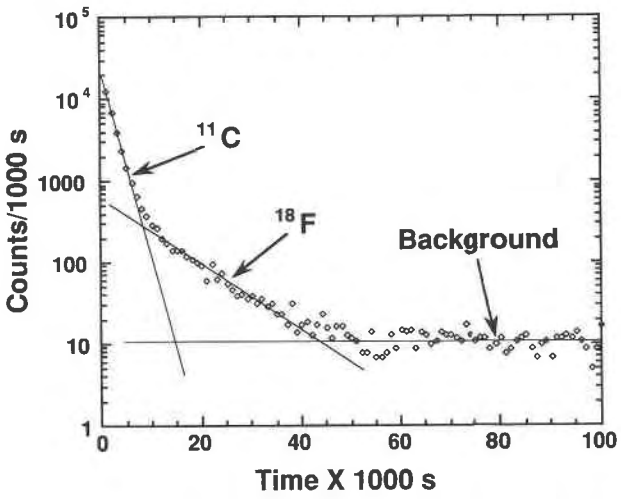

Fig. 1. The decay activity for diamond activated with a beam of ^{3}He of 4.5 MeV energy. The steep segment is due to decay originating from ^{12}C activation, and the intermediate segment from decay originating from ^{16}O activation. Superimposed on these is a flat background of ≈11 counts/10^3 s. The form of the curve is described by Eq. 4, the coefficients of which are determined by a nonlinear least-squares regression procedure.

of the large variation of cross section with energy is that the analytical sensitivity decreases rapidly with depth. The practical analytical depth in diamond is ≈8 μm, which is the depth below the surface where the energy of a $^3He^{2+}$ particle initially of 4.5 MeV is reduced to <2 MeV (Fig. 2B). Typical beam diameters used for activation were 300–800 μm (see below), and so beam diameter essentially determines analytical resolution.

To determine concentration it is necessary to refer the unknown to a standard (std). Using Al_2O_3 (0.6 atomic fraction O) for this purpose, the total analytical expression is

$$C_d = 0.6(y_d/y_{std})(Q_{std}/Q_d)[\int \phi_{std}(x)\,dx/\int \phi_d(x)\,dx]. \quad (7)$$

It was not possible to measure Q directly because of the analytical design (see below). Instead a particle backscatter spectrum was obtained for every activation. The intensity of the spectrum for a particular composition target is proportional to and serves as an indirect measure of Q. The backscatter spectra of the diamond unknowns were normalized to each other. In order to relate the Q of diamond activations with those of standard activations, an initial calibration of the spectra of the two targets was performed. This was accomplished by normalizing spectra from the two targets to the backscatter intensity of a pure Au layer that had been deposited on each.

O on diamond surfaces determined by RBS

Either accounting for or eliminating O adsorbed on the analytical surface determined the design of our experiments. For this reason, characterizing the diamond surface was an important part of our initial work. Two sources of O were discovered. The first, as expected, was that

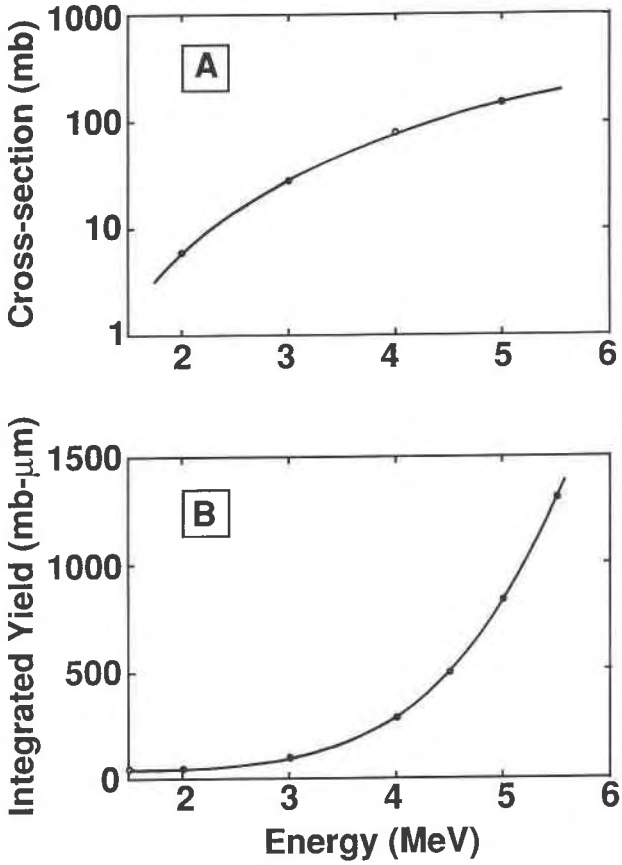

Fig. 2. (**A**) Variation of the cross section of Reaction 2 as a function of ^{3}He energy. (**B**) The integrated cross section in terms of millibarns per micrometer of Reaction 2 in diamond as a function of ^{3}He energy. At 4.5 MeV $\int \phi_{Al_2O_3}(x)\,dx$ = 520 and $\int \phi_d(x)\,dx$ = 490 mbarn/μm.

adsorbed from the atmosphere before the sample was introduced into the vacuum chamber. The second was a contamination that built up on the surface during activation (see below). Diamond surfaces were analyzed by Rutherford backscattering spectrometry (RBS) (e.g., Chu et al., 1978). Although RBS is most sensitive for heavy elements because the elastic scattering cross sections for α particles increase with Z, elements heavier than O are not present in diamond, and therefore no background is associated with the O signal in the RBS spectrum. In practice, slit scattering causes a small (≪1%) proportion of the incident particles to fall beyond the nominal beam, and thus there is usually a small backscattered signal from the metal sample holders. The magnitude of this stray signal, together with that due to pulse pile-up, determine the RBS O detection limit, which was found to be ≈0.4 × 10^{15} atoms/cm^2 (3σ level). Surface concentrations were computed from spectral intensity data and from simulations constructed from the program Rump (Doolittle, 1985).

The diamond samples were prepared for RBS analysis by simply rubbing by hand previously polished surfaces

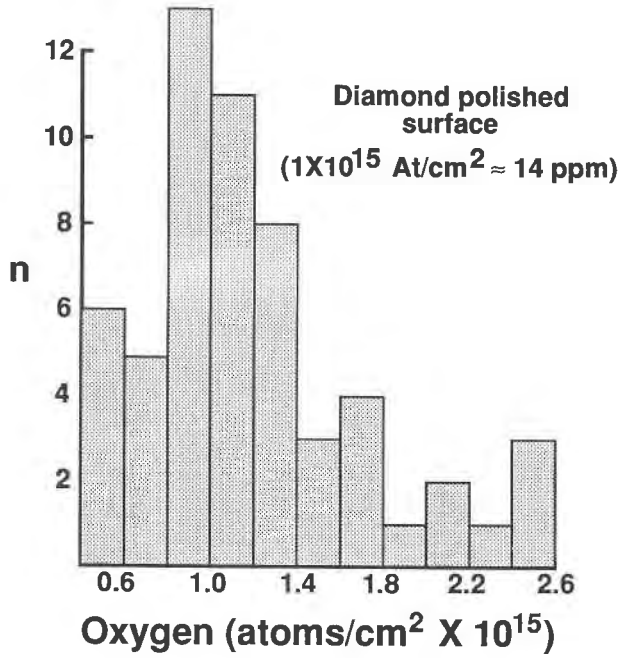

Fig. 3. Histogram of O concentrations on diamond surfaces determined by Rutherford backscatter spectrometry (see text).

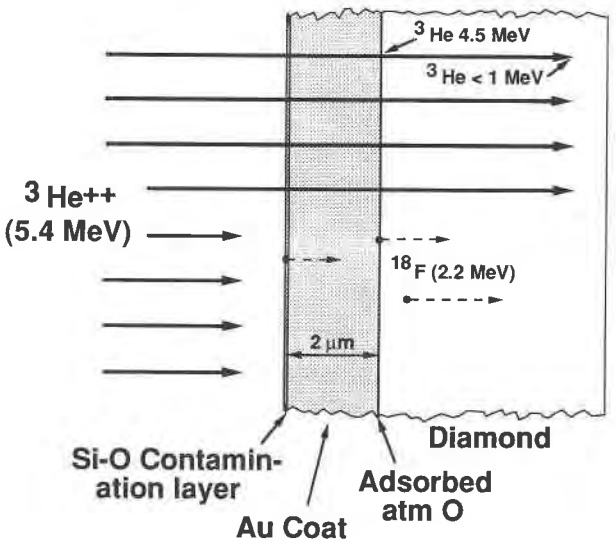

Fig. 4. The configuration of diamond targets in the microbeam experiments. A layer of Au 2 μm thick was deposited on the diamond samples to trap O-rich contaminants, which build up on the analytical surface during bombardment.

on a thickly napped cloth charged with 15 μm of diamond paste. (Cleaved surfaces were also examined, but elements other than C were frequently observed in their RBS spectra.) The samples were cleaned ultrasonically in successive acetone and methanol baths for 10–15 min, pressed into In on the sample holder, and introduced into the vacuum chamber. The ambient pressure during experiments was $\approx 5 \times 10^{-7}$ torr and was maintained by cryogenic pumping. Neither the cleaning procedures nor the length of time samples were exposed to atmosphere was found to have any significant effect on the amount of adsorbed surface O.

Figure 3 is a histogram of the amounts of O on polished diamond surfaces obtained by RBS analysis. It is seen that surface O concentrations were typically $< 1.4 \times 10^{15}$ atoms/cm^2. Higher concentrations were accompanied by peaks associated with other elements or by observable residues. As a consequence, it was assumed that adsorbed surface O contributes a maximum of 10^{15} atoms/cm^2, which is equivalent to 14 ppm in the bulk analysis obtained by activation. This amount also represents a continuous monolayer of surface O. O is also the only detectable contaminant in Auger electron spectroscopic (AES) studies of polished diamond surfaces (Pate, 1986). (H is surely present but not detected by AES or RBS.) As exposure of diamond to the atmosphere is not known to result in the formation of a bulk oxidized phase (Pate, 1986), a monolayer of O due to adsorption is believed to represent an upper limit, and higher concentrations are due to contamination.

Experimental design

Some of our experiments were carried out in the nuclear microprobe. This is a beam line fitted with a superconducting solenoid, which provides for the focusing of energetic, high-current beams of light ions to spot sizes of < 10 μm (Maggiore, 1980). Unfortunately, it was found that an O-Si contamination layer builds up over time on the target surface during particle bombardment. This unexpected contaminant, the source of which is unknown but is apparently from the accelerator itself, proved troublesome because it typically added several hundred parts per million O to the analysis. The ^{18}F nucleus produced by Reaction 2 is imparted an energy of 2.2 MeV. Thus, ^{18}F produced at the surface does not remain there but becomes implanted in the diamond to depths of ≈ 1 μm and cannot be removed. The elimination of this contamination determined the design of our experiments.

In most experiments, diamond samples were activated for 1.5–2 h at beam currents of 10–20 nA. Because of the complexity of the problem, two types of experiments were conducted as a check on the validity of the results.

Microbeam experiments

In the first set of experiments, diamond samples were coated before activation with a layer of Au 2 μm thick (produced by RF magnetron sputter deposition). A Au layer of this thickness serves to trap the contaminant reaction product, according to calculations of stopping power with Trim (Ziegler et al., 1985). The resulting configuration of the sample and various sources of O are illustrated in Figure 4.

A complexity introduced by the Au is the fact that the

incident beam loses energy as it penetrates the Au. Thus, the thickness of the layer must be known precisely in order that the energy of ^{3}He as it reaches the diamond surface is known. Au coat thicknesses were measured by RBS, and an incident beam energy of 5.4 MeV was used to obtain 4.5 MeV ^{3}He at the diamond surface (Fig. 4).

After activation and before counting, the Au coat along with trapped contaminants were removed by polishing for several minutes on a thickly napped cloth with 15 μm of diamond paste. After the diamond samples were counted, their surfaces were reexamined by RBS to confirm that all Au had been removed. Obviously, this procedure does not eliminate the O that was initially on the surface before Au deposition. Before Au deposition the diamond samples were cleaned by the procedure described above. Based on the previous RBS experiments, it was assumed simply that a monolayer of O was trapped beneath the Au layer, and therefore 14 ppm O was subtracted from all the analyses.

The reason that this complex procedure was adopted was that it allowed analysis with the microbeam and thus the investigation of small diamond samples (<1 mm). The analytical region in these experiments was $\approx 300 \times 8$ μm, but, more importantly, microscopic control of beam positioning was possible. However, the advantage in spatial resolution was offset by the complexity of the experiment and its inherent uncertainties.

The most important uncertainty is the possibility that the Au layer itself may have contained small quantities (tens of parts per million) of O. The RBS spectra of the Au coats contained no evidence of included contaminants. However, because the O signal rests on a high background consisting of particles backscattered from Au, the method applied to high Z targets is probably not sensitive enough to detect O concentrations below several hundred parts per million, and so no means exist to evaluate this possibility. A constant O background from the Au does not account for the observed variability of O content. Therefore, we have no reason to suspect that the Au contained O but we also cannot rule it out. A second source of error is the O on the diamond surface trapped beneath the Au coat. As noted above, it was assumed that surface O contributed 14 ppm to the analysis, but as the RBS data in Figure 3 illustrate, the amount of surface O may not be constant. Both potential sources of error in the microbeam experiments would contrive to cause the O content of diamond to be overestimated.

Broad-beam experiments

In the second set of experiments, diamond surfaces were sputtered with Ar^+ for 10–15 min immediately prior to and then continually during activation, which presumably eliminated completely the problem of surface O. Ar^+ energies of 4 keV and beam currents of 300–500 nA were used to bombard regions 5–15 mm across to ensure that the ^{3}He beam fell entirely within the sputtered region. The sputtering rate of diamond is not known precisely for these conditions. Therefore, a series of RBS experiments was conducted to establish that O adsorbed on the surface was completely removed from the diamond surfaces after 10 min of sputtering and that the surfaces remained clean during prolonged ^{3}He bombardment. Some of the diamond must have been removed as well during the ≈ 2 h of continuous sputtering. Although the removal of 10^2–10^3 Å of the diamond surface would not significantly influence the results, in contrast to the microbeam analyses, the broad-beam analyses represent minimum O contents.

Because of the proximity of the superconducting solenoid and the intense magnetic field it produces, it is not physically possible to operate the sputtering apparatus in the sample chamber of the microbeam line. Instead a general purpose chamber was used, in which the ^{3}He beam was focused by a quadrupole lens and collimated to a final diameter of 750–850 μm. Although the beam diameter was relatively well defined, it was not possible to observe samples microscopically, and so precise placement of the beam on the target was not possible. In practice, it was found that this limited us to examination of diamond surfaces ≥ 2 mm across.

Precision and accuracy of measurements

There are two primary sources of error in the O analyses. The first one resides in the measurement of the total charge (Q in Eqs. 6, 7) of the activating beam on standards and unknowns. As noted above, the charge is measured indirectly from the intensity of a specific region of the backscatter spectrum collected during activation. In theory it is subject only to counting error, which was $\approx 1.4\%$ (2σ) for a typical analysis. In practice, however, it appears to be much larger when estimated from repeated analyses of the alumina standard. Comparison of the standards indicates a 2σ precision of $\approx 10.4\%$.

A second source of error is in the fitting of the decay activity curves (Fig. 1). For the standards this was negligible. For the diamond samples, the error in computing B in Equation 4 was found to be dependent on the O content and ranged from 16% for a diamond sample containing 12 ppm to 9% for one having 95 ppm O (samples G100364 and J798, respectively, in Table 1). The total error for most analyses in Table 1 is thus estimated to be in the range of 14–19% (relative) (2σ).

The accuracy of the analyses is determined by those of the standard composition and matrix correction, both of which are well known. The analyses are similarly accurate.

Results

The results from the microbeam and broad-beam experiments are presented in Table 1. For the 28 diamond samples analyzed, O contents range from 5 to 373 ppm. Most of the samples contain <100 ppm O, with only two containing >120 ppm. The analyses listed in Table 1 are for spots that upon careful microscopic examination were

Table 1. O contents of diamond samples determined by two different microactivation experiments

Sample	Type	Description	O (ppm atomic)	
			Microbeam	Broad beam
D7	IIa		92	
D8	IIa		84	
D11	IIa		78	
D16	IIa		16	
D20	IIa		50	
D21	IIa		51	
D22	IIa		102	
D23	IIa		37	
D24	IIa		95	109
D27	IIa			29
D28	IIa			42, 39
D29	IIa			22
D30	IIa			23
D31	Ia			15
D32	Ia			25
D3a	IaA (≈30% B)	Muji Mayi	116	
OR2	IaA (≈40% B)	Orapa, eclogitic incl.	49	
OR3	IaB	Orapa, eclogitic incl.		274
OR10	I	Orapa, eclogitic incl.	65	
J746	Ia	Finsch, eclogitic incl.		25
J787	IaB (≈40% A)	Finsch, eclogitic incl.		41
J798	IaA	Finsch, eclogitic incl.		95, 99
BRAZ2	IIa			373, 31
BRAZ5	IIa			5
G100364	IaB	Argyle, pale purple		12
A4-03	Ia	Monastery, moissanite incl.	75	
A1-15	Ia	Monastery, moissanite incl.	102	
G100363	Ia	Sumitomo, synthetic yellow		49, 58

found to be free of inclusions, microcracks, and other defects.

One diamond sample (D24) was analyzed by the two procedures. The microbeam experiment yielded an O content of 94 ppm and the broad-beam experiment 109 ppm. The two analyses are well within experimental error, giving us confidence that the microbeam experiments are correct and that O was not trapped in the Au layer. Four diamond samples were analyzed twice by the broad-beam technique (Table 1). Three of the four analyses also fell well within experimental error of each other. The two analyses of the sample BRAZ2 differed by an order of magnitude. This difference is believed to be real and is discussed below.

The 11 analyzed type IIa diamond samples are 1 or 2 mm square, doubly polished plates purchased commercially, and from unknown localities. They are colorless and devoid of mineral or fluid inclusions detectable by optical microscopy and exhibit strong birefringence. Type IIa diamond samples are characterized by the absence of N, B, H, or other impurities detectable in IR spectra, and for this reason it was initially anticipated that they would also contain little or no O. It can be seen, however, that they typically contain several tens of parts per million O.

Among the other samples analyzed were type Ia, as well as other type IIa, diamond samples (Table 1). Two of these (D31 and D32) are also inclusion free, colorless platelets purchased commercially. Both were found to possess relatively low O contents. Most of the other diamond samples contain visible inclusions and microcracks. These were avoided, and analyses in which the beam was inadvertently placed on such features were rejected. Some of the diamond samples are fragments of larger stones from which mineral inclusions had been removed, as indicated.

Samples A4-03 and A1-15 from the Monastery kimberlite are particularly noteworthy. These are fragments of stones from which moissanite (SiC) inclusions had been extracted. Moissanite is stable only under highly reducing conditions, the maximum stability in terms of f_{O_2} being about five orders of magnitude below that of the Fe + wüstite buffer under all conceivable *PTX* conditions of the upper mantle (Eggler and Lorand, 1991). That A4-03 and A1-15, which were found to contain 75 and 102 ppm O, respectively, are not highly depleted in O compared with the other diamond samples (Table 1) indicates either that the diamond and moissanite did not form under the same f_{O_2} conditions or that the O content of the diamond is controlled by factors in addition to strictly thermodynamic ones.

A synthetic diamond sample (G100363) was also analyzed. Its canary yellow color is typical of synthetic diamond in which N substitutes for C. The sample is a polished cube approximately 2 mm across containing numerous microscopic inclusions. Although the specific synthesis process is not known, most of such diamond is produced by precipitation from a transition metal melt, implying formation under reducing conditions. Yet this diamond sample too was found to contain O (≈50 ppm).

Finally, it is necessary to return to the case of BRAZ2, the two analyses of which gave variable results. The analyzed region that yielded 373 ppm O was examined op-

tically and found to be free of inclusions, microcracks, or other defects at the limit of optical resolution. However, it was also observed that a microcrack deeper in the sample projected into that region. The second analysis, which yielded only 31 ppm O, was of a different region, far removed from any such feature. It is concluded that O detected in the first analysis most likely resides in a microfracture or inclusion array that is optically invisible. Other elements were sought by electron microprobe but not detected in the O-rich region of BRAZ2 (see below), implying that, if O is in the microfracture or inclusion array, it is present as CO_2 or H_2O.

TEM investigation

Two type IIa diamond samples were examined by transmission electron microscopy (TEM) to determine whether dislocation densities are sufficiently high to account for the measured O. These were obtained as wafers 20 μm thick to facilitate making foils, but, because of the difficulty of handling, they were not analyzed for O. The wafers were mounted on slotted Cu grids and thinned to perforation on a Gatan ion miller. Final thinning was performed using liquid N_2 and a low-angle beam to minimize radiation damage. They were examined with a Philips CM30 instrument operated at 300 kV.

Both (001) and (110) wafers were examined. Standard $\mathbf{g}\cdot\mathbf{b}$ analysis was used to determine the Burgers vectors $\mathbf{b}$ ($\mathbf{g}$ = operating diffraction vector), and dislocation line directions were determined by trace analysis. The dislocation structure of both samples is similar and typical of deformed material, with no indication of recovery by climb. The Burgers vectors of the dislocations are all six $\frac{1}{2}\langle 110\rangle$ type, which is expected since this is the shortest lattice vector. The dislocations tend to lie along $\langle 110\rangle$ directions with a 60° angle to the Burgers vectors, as commonly observed for substances having the diamond cubic structure. Many of the dislocations are in the form of dipoles consisting of dislocations of opposite sign. Weak beam dark-field microscopy shows that the dislocations are dissociated into Shockley partials, with a separation of ≈30–40 Å. The samples exhibit a mosaic structure consisting of regions of low dislocation density (cells) surrounded by regions of high dislocation density (cell walls). The structure, which is typical of type IIa diamond, apparently forms as a consequence of plastic deformation and causes the marked birefringence characteristic of type II diamond (e.g., Lang, 1979, Fig. 14.4).

The average dislocation density, which was determined by counting the number of intersections with the foil surfaces, was found to be $\rho \approx 2 \times 10^{13}/m^2$. This is somewhat higher than the dislocation density Lang (1979) guessed to be typical, on the basis of observations of cathodoluminescence. Suppose that each atomic plane along the dislocations can carry n segregated O atoms. The separation of the atomic planes is $a/\sqrt{2}$, where a is the lattice parameter of the diamond. The number of O atoms per unit volume is then $(n\rho\sqrt{2})/a$. The number of C atoms per unit volume is $8/a^3$, so for $\rho = 2 \times 10^{13}/m^2$ and a = 0.357 nm, the fractional concentration of O is $C_d = (n\rho a2)/4\sqrt{2} \approx 0.5 \times 10^{-6}n$. If the dislocation core is undissociated and saturated with O, n could be about 2, in which case $C_d \approx 1$ ppm. If the dissociation of dislocations is taken into account, the stacking fault area could be saturated, giving $n \approx 10$–20 and $C_d \approx 5$–10 ppm. No bubbles or platelets were observed down to the limit of resolution of about 10 Å. Bearing in mind that the small regions of two diamond samples examined by TEM may not be representative, one can observe that there are not enough dislocations in the type IIa diamond samples for all the O to be resident in them.

FTIR spectroscopy

Diamond samples were analyzed by micro-Fourier transform infrared (FTIR) spectroscopy to determine (or confirm) diamond type (Table 1) and to search for the presence of vibrational bands that could be attributed to O in the diamond structure. Diamond spectra were obtained at Bell Laboratories (Murray Hill, New Jersey) using a Digilab FTS-60 configured with a microscope housing an MCT detector cooled with liquid N_2. The useful spectral region of the detector is the mid-IR between 4500 and 650 cm^{-1}. Spectra were acquired using a resolution of 2 or 4 cm^{-1} and 128, 256, or 512 scans. The microscope is equipped with a 36× lens with an adjustable rectangular aperture allowing sampling to spot sizes as small as 10 μm. In general, spot sizes of ≈100 μm were used, and areas free of inclusions were selected for analysis.

The diamond classification based on the IR results is presented in Table 1. The N platelet peak located between 1390 and 1348 cm^{-1} (Taylor et al., 1990) was present in most of the type Ia diamond samples. For example, all three Finsch diamond samples contained the platelet band, and in J787 it was far more intense than the B bands of N. Several bands attributable to H (Woods and Collins, 1983), such as the C-H stretching band at 3107 cm^{-1}, were observed in several type I diamond samples. The spectra of the natural Orapa OR2 and synthetic Sumitomo samples also displayed bands representing N-H stretching (Woods and Collins, 1983).

The FTIR spectra of both type I and II diamond were scrutinized for the presence of bands attributable to the presence of O. The spectral regions of particular interest were molecular CO_2 (2350 cm^{-1}), molecular CO (2160 cm^{-1}), carbonyl (2125–1700 cm^{-1}), and carbonate (1700–1300 cm^{-1}). Subtraction spectra of type IIa diamond were also produced to accentuate O bands of low intensity. This method was used specifically with type IIa diamond samples since they contain very low levels of N and thus interfering N bands (1400–900 cm^{-1}) or any influence N may have on the lattice vibrational bands (5000–1500 cm^{-1}) were minimized. No bands attributable to O were found in either the pure or subtraction spectra.

Although IR bands have been associated with O adsorbed on diamond powders (Sappok and Boehm, 1968a, 1968b), Davies (1977) reported that no optical evidence

had been found for the presence of O (or Si, Mg, Fe, and Ca) in the diamond structure. Further, he stated that when trace-element concentrations of ≈100 ppb are exceeded, an optically active vibration should be present in the diamond spectrum. Part of the difficulty in evaluating the plausibility of this extremely low detection limit is that the extinction coefficients of the bands of interest are unknown. Additionally, the extinction coefficients differ for each band; thus, the detection limit will vary with both the element causing the vibration and the nature or symmetry of the molecular structure of the impurity. The detection limit is also dependent on specimen thickness, as per the Beer Lambert law $C = 10^6 \cdot MW \cdot \text{Abs}/\rho \cdot \epsilon \cdot d$ where C is concentration (in parts per million weight), MW is molecular weight of O (16 g/mol), Abs is absorbance (dimensionless), ρ is density of diamond (3.4 g/cm^3), d is the specimen thickness (in centimeters), and ϵ is the extinction coefficient (in squared centimeters per mole).

Although the extinction coefficients of probable C-O vibration bands are unknown, an upper limit can be placed on their value for a given thickness and concentration at minimum detection. For example, with Abs = 0.001 and d = 0.5 mm (the thickness of several of our type IIa samples), the inversion of Beer's law yields a maximum extinction coefficient of 10^3 cm^2/mol, for a detection limit of 100 ppm O. In comparison, carbonate and molecular CO_2 dissolved in silicate melts have extinction coefficients of $\approx 10^5$ and 10^6 cm^2/mol, respectively (Fine and Stolper, 1985), and that of N in diamond is $\approx 10^5$ cm^2/mol (Kaiser and Bond, 1959). If the latter value is taken as a crude approximation for the extinction coefficient of an O band in diamond, the detection limit of O present as various functional groups with C is anticipated to be ≈500 ppb. These considerations suggest that O is not bonded to C in the diamond structure.

Electron probe analysis

To determine whether O in the O-rich samples D24, J798, OR-3, and BRAZ2 is contained in submicroscopic inclusions of other phases, the same spots analyzed for O were first examined by scanning electron microscopy for surface imperfections and the presence of other phases and then analyzed by electron probe for Al, Si, K, Fe, and Mg. The ^{3}He beam leaves a dark spot caused by radiation damage, so the analyzed regions are easily reoccupied. Electron probe analyses were conducted with an ARL SEMQ instrument using the standard WDS spectrometers. Conditions of high beam currents, long count times, and appropriate electronic filtering of the signal were employed such that detection limits of <15 ppm (wt) for Si and K and <30 ppm for the other elements were achieved. None of the five elements was detected in the diamond samples.

O IN DIAMOND

Since there is more O than can be accommodated by dislocations in at least the type II diamond, it is necessary to consider possible mechanisms of O incorporation. Diamond is cubic, with space group $Fd3m$. The C atoms are arranged in tetrahedra, reflecting the sp^3 hybrid state of the C-C bond. Thus, the coordination is only fourfold, compared with the 12-fold coordination that would exist in a structure of closest packed spheres of the same size, as exhibited, for example, by some metals. As a consequence, the diamond structure is relatively open, with only 34% of the available space occupied. In fact, the unit cell can be thought of as consisting of eight octants, four of which are filled with C tetrahedra and four of which are empty (Gildenblat et al., 1991). The interatomic distance is 1.54 Å, and so from a geometric point of view the unit cell can accommodate eight extra spheres of diameters 1.54 Å in the interstitial positions. The electronic structure of O probably prohibits it from a strictly substitutional role in the diamond structure, and, as noted above, that is indicated by the IR evidence. However, the atomic radius of O (0.65 Å) is similar to the covalent radius of C (0.77 Å). It is conceivable, therefore, that small amounts of O, perhaps in partly aggregated states, may occupy the interstitial positions with only limited deformation of the lattice.

Although examples of nearly perfect crystals are known, many individual diamond samples exhibit large variations in abrasion resistance, impurity levels, and other properties. Frank et al. (1990) reported differences in N concentrations of 25–30% within portions of individual cubic growth sectors in synthetic, yellow type Ib (singly substituted N) diamond. They attributed the differences to preferential N incorporation at different locations on the surface during growth, with N being preferentially incorporated on the vicinal slopes of the growth pyramids. Such phenomena are reported to be common in faceted growth. For example, Smet and van Enckevort (1988) described Bridgman-grown bismuth germanate crystals that display large differences in defect segregations in adjacent growth sectors. They argued that defect segregation is governed by surface kinetic factors rather than by the equilibrium bulk defect distribution. This suggests that the impurity contents of diamond may have little to do with ambient thermodynamic properties, such as O activity, of the systems in which they grew. The large quantities of O found in the diamond from which moissanite inclusions had been removed is consistent with the diamond surface exerting an important control on the incorporation of O in the crystal during growth. We hypothesize that the O content of diamond is controlled by crystal surface properties during growth rather than by only equilibrium thermodynamic conditions and the bulk-crystal equilibrium defect structure.

ACKNOWLEDGMENTS

This paper has benefited from the critical reviews of Henry Meyer, Emmanual Fritsch, Alan Collins, and Jeff Harris. We thank Rory Moore and John Gurney for supplying diamond samples from which specific mineral inclusions had been extracted, Jeff Harris for samples from known localities and for arranging for some to be polished, and Rick Hervig and Robert Wilson for their attempts to analyze diamond by SIMS. We are indebted to Los Alamos inmates Joe Tesmer, Mark Hollander, and Caleb

Evans for operating the accelerator and helping to set up the experiments and to Joe Martin for solutions to some of the diamond surface problems. We also thank Coralie Pryde and Maureen Chan of Bell Labs, Murray Hill, for providing access to the IR equipment. The financial support of U.S. Department of Energy and NSF grant EAR-89-03645 (to E.A.M.) are gratefully acknowledged.

References cited

Bibby, D.M. (1982) Impurities in natural diamonds. In P.A. Thrower, Ed., Chemistry and physics of carbon, vol. 18, p. 1–91. Marcel Dekker, New York.

Borders, J.A., and Harris, J.M. (1978) The use of $^{12}C(d,p)^{13}C$ and $^{16}O(d,p)^{17}O$ reactions to profile carbon and oxygen in solids. Nuclear Instruments and Methods, 149, 279–284.

Chu, W.-K., Mayer, J.W., and Nicolet, M.-A. (1978) Backscattering spectrometry, 384 p. Academic, New York.

Davies, G. (1977) The optical properties of diamond. In P.A. Thrower and P.L. Walker, Jr., Eds., Chemistry and physics of carbon, vol. 13, p. 1–143. Marcel Dekker, New York.

Deines, P. (1980) The carbon isotopic composition of diamonds: Relationship to diamond shape, color, occurrence and vapor composition. Geochimica et Cosmochimica Acta, 44, 943–961.

Doolittle, L.R. (1985) Algorithms for the rapid simulation of Rutherford backscattering spectra. Nuclear Instruments and Methods, B9, 344–351.

Eggler, D.H., and Baker, D.R. (1982) Reduced volatiles in the system C-O-H: Implications to mantle melting, fluid formation, and diamond genesis. In S. Akimoto and M.H. Manghanani, Eds., High-pressure research in geophysics, p. 237–250. Reidel, Dordrecht, The Netherlands.

Eggler, D.H., and Lorand, J.P. (1991) Sulfides, diamonds, and mantle f_{O_2}. In Proceedings of the 5th International Kimberlite Conference, Araxa, Brazil, Extended Abstracts, p. 88–91. Companhia de Pequisa de Recursos Minerais, Rio de Janeiro, Brazil.

Fine, G., and Stolper, E. (1985) The speciation of carbon dioxide in sodium aluminosilicate glasses. Contributions to Mineralogy and Petrology, 91, 105–121.

Frank, F.C., Lang, A.R., Evans, D.J.F., Rooney, M.-L.T., Spear, P.M., and Welbourn, C.M. (1990) Orientation-dependent nitrogen incorporation on vicinals on synthetic diamond cube growth surfaces. Journal of Crystal Growth, 100, 354–376.

Galimov, E.M. (1991) Isotope fractionation related to kimberlite magmatism and diamond formation. Geochimica et Cosmochimica Acta, 55, 1697–1708.

Gildenblat, G.S., Grot, S.A., and Badzian, A. (1991) The electrical properties and device applications of homoepitaxial and polycrystalline diamond films. Proceedings of the IEEE, 79, 647–667.

Graham, J., and McKenzie, C.D. (1987) Oxygen in pyrrhotite. II. Determination of oxygen in natural pyrrhotites. American Mineralogist, 72, 605–609.

Green, D.H., Falloon, T.J., and Taylor, W.R. (1987) Mantle-derived magmas: Roles of variable source peridotite and variable C-O-H fluid compositions. In B.O. Mysen, Ed., Magmatic processes: Physicochemical principles, p. 139–154. The Geochemical Society Special Publication, University Park, Pennsylvania.

Kaiser, W., and Bond, W.L. (1959) Nitrogen, a major impurity in common type I diamond. Physical Review, 115, 857–863.

Lang, A.R. (1979) Internal structure. In J.E. Field, Ed., Properties of diamonds, p. 425–469. Academic, London.

Leung, I. (1990) Silicon carbide cluster entrapped in a diamond from Fuxian, China. American Mineralogist, 75, 1110–1119.

Maggiore, C. (1980) Materials analysis with a nuclear microprobe. Scanning Electron Microscopy, 1, 439–454.

Meyer, H.O.A., and McCallum, M.E. (1986) Mineral inclusions in diamonds from the Sloan kimberlites. Journal of Geology, 94, 600–612.

Moore, R.O., and Gurney, J.J. (1985) Pyroxene solid solution in garnets included in diamond. Nature, 318, 553–555.

Moore, R.O., Otter, M.L., Rickard, R.S., Harris, J.W., and Gurney, J.J. (1986) The occurrence of moissanite and ferro-periclase as inclusions in diamond. In Proceedings of the Fourth International Kimberlite Conference Abstracts, Perth, Western Australia, Australia.

Pate, B.B. (1986) The diamond surface: Atomic and electronic structure. Surface Science, 165, 83–142.

Richardson, S.H., Gurney, J.J., Erlank, A.J., and Harris, J.W. (1984) Origin of diamonds in old enriched mantle. Nature, 310, 198–202.

Sappok, R., and Boehm, H.P. (1968a) Chemie der Oberfläche des Diamanten. I. Benetzungswärmen, Elektronenspinresonanz und Infrarotspektren der Oberflächen-Hydride, -Halogenide und -Oxide. Carbon, 6, 283–295.

——— (1968b) Chemie der Oberfläche des Diamanten. II. Bildung, Eigenschaften und Struktur der Oberflächenoxide. Carbon, 6, 573–588.

Sellschop, J.P.F. (1979) Nuclear probes in physical and geochemical studies of natural diamonds. In J.E. Field, Ed., The properties of diamond, p. 107–163. Academic, New York.

Sellschop, J.P.F., Annegarn, H.J., Keddy, R.J., Madiba, C.C.P., and Renan, M.J. (1978) Ion beam analyses in relation to the physical properties of diamond. Nuclear Instruments and Methods, 149, 321–328.

Sellschop, J.P.F., Madiba, C.C.P., Annegarn, H.J., and Shongive, S. (1979) Volatile light elements in diamonds. Diamond Research, 24–30.

Sellschop, J.P.F., Madiba, C.C.P., and Annegarn, H.J. (1980) Light volatiles in diamond: Physical interpretation and genetic significance. Nuclear Instruments and Methods, 168, 529–534.

Smet, F., and van Enckevort, W.J.P. (1988) On the distribution of point defects in large sized bismuth germanate crystals. Journal of Crystal Growth, 88, 169–179.

Taylor, W.R., and Green, D.H. (1987) The petrogenetic role of methane: Effect on liquidus phase relations and the solubility mechanism of reduced C-H volatiles. In B.O. Mysen, Ed., Magmatic processes: Physicochemical principles, p. 121–138. The Geochemical Society Special Publication, University Park, Pennsylvania.

Taylor, W.R., Jaques, A.L., and Ridd, M. (1990) Nitrogen-defect aggregation characteristics of some Australasian diamonds: Time-temperature constraints on the source regions of pipe and alluvial diamonds. American Mineralogist, 75, 1290–1310.

Woods, G.S., and Collins, A.T. (1983) Infrared absorption spectra of hydrogen complexes in type I diamonds. Journal of Physics and Chemistry of Solids, 44, 471–475.

Ziegler, J.F., Biersack, J.P., and Littmark, U. (1985) Stopping and ranges of ions in matter. Pergamon, New York.

Manuscript received July 20, 1992
Manuscript accepted March 17, 1993